IMPROVED SURROGATE-BASED OPTIMIZATION OF A MARINE ECOSYSTEM MODEL USING RESPONSE CORRECTION

M. Prieß[1], S. Koziel[2] and T. Slawig[1]

[1]*Institute for Computer Science, Cluster The Future Ocean, Christian-Albrechts Universität zu Kiel, 24098 Kiel, Germany*
[2]*Engineering Optimization & Modeling Center, School of Science and Engineering, Reykjavik University*
Menntavegur 1, 101 Reykjavik, Iceland

Keywords: Climate models, Marine ecosystem models, Surrogate-based optimization, Parameter optimization, Response correction.

Abstract: An improved surrogate-based optimization (SBO) methodology is developed for the optimization of climate model parameters. Our technique is based upon a multiplicative response correction technique to create a surrogate from a temporarily coarser discretized physics-based low-fidelity model. The original version of this methodology was successfully applied to calibration of a (one-dimensional) representative of a class of marine ecosystem models yielding about 84% computational cost savings when compared to the high-fidelity model optimization. Here, we demonstrate that by employing relatively simple modifications of the response correction scheme, the surrogate model accuracy and the efficiency of the optimization process can be further improved. More specifically, for the considered test case, the optimization cost is reduced three times when compared to the original technique, i.e., from about 15% to only 5% of the cost of the direct high-fidelity ecosystem model optimization (used as a benchmark method). The corresponding time savings are increased to 95%.

1 INTRODUCTION

Surrogate-based optimization (SBO) (Queipo et al., 2005) is a methodology to efficiently optimize complex, so-called *high-fidelity* models, that require substantial computational effort already for a model evaluation. High-fidelity models are typically evaluated through computer simulation and evaluation times of several hours, days or even weeks are not uncommon. As a consequence, optimization and control problems for such models are often still beyond the capability of modern numerical algorithms and computer power. The idea of SBO is to exploit a surrogate, a computationally cheap and yet reasonably accurate representation of the high-fidelity model. The surrogate replaces the high-fidelity model in the optimization process in the sense of providing predictions of the model optimum. Also, it is updated using the high-fidelity model data accumulated during the process. The prediction-updating scheme is normally iterated in order to refine the search and to locate the high-fidelity model optimum as precisely as possible. One of possible ways of creating the surrogate, our work in this paper is based on, is to utilize a physically-based *low-fidelity* model.

SBO is widely and very successfully used in engineering sciences (Bandler et al., 2004; Forrester and Keane, 2009; Leifsson and Koziel, 2010; Queipo et al., 2005). The application on parameter optimization in climate models is new.

Climate models are typically given as time-dependent partial differential or differential algebraic equations (PDEs/DAEs) (Majda, 2003; McGuffie and Henderson-Sellers, 2005; Gill, 1982). One example are marine ecosystem models (Fennel and Neumann, 2004; Sarmiento and Gruber, 2006), one of which our work in this paper is based on. Marine ecosystem models describe photosynthesis and other biogeochemical processes in the marine ecosystem that are important, e.g., to compute and predict the oceanic uptake of carbon dioxide (CO_2) as part of the global carbon cycle (Sarmiento and Gruber, 2006). Since the number of processes that have to be included and the needed temporal and spatial resolution is quite high, so is the computational effort.

The aim of parameter optimization is to adjust or identify the model parameters such that the model response fits given measurement data (Banks and Kunisch, 1989). The mathematical task thus can be classified as a least-squares type optimization or inverse

problem (Tarantola, 2005).

This optimization (or calibration) process requires a substantial number of (typically expensive) function and optionally sensitivity or gradient or even Hessian matrix evaluations. Hence, decreasing the effort related to the function evaluations (or, equivalently, cutting down the number of function calls necessary to find the optimum) is of primary importance to reduce the overall optimization cost. This becomes particularly significant for computationally expensive three-dimensional coupled models, for example, global climate models (Gill, 1982).

In (Prieß et al., 2011), a surrogate-based methodology has been developed for the optimization of climate model parameters. The technique is based upon a multiplicative response correction technique to create a surrogate from a temporarily coarser discretized physics-based low-fidelity model. It has been successfully applied to a (one-dimensional) representative of a class of marine ecosystem models and demonstrated to yield substantial savings of the computational cost of the optimization process when compared to a direct optimization of the high-fidelity model.

In this paper, we demonstrate that by employing simple modifications of the original response correction scheme, one can improve the surrogate's accuracy, as well as further reduce the computational cost of the optimization process. We verify our approach by using synthetic target data and by comparing the results of SBO with the improved surrogate to those obtained with the original one. The optimization cost is reduced three times when compared to previous results, i.e., from about 15% to only 5% of the cost of the direct high-fidelity ecosystem model optimization (used as a benchmark method). The corresponding time savings are increased to from 84% to 95%.

The paper is organized as follows. The high-fidelity ecosystem model, considered here as a test problem, as well as a low-fidelity counterpart that we use as a basis to construct the surrogate model, are described in Section 2. The optimization problem under consideration is formulated in Section 3. The original and improved response correction schemes and the comparison of the corresponding surrogate model qualities are discussed in Section 4. Numerical results for an illustrative SBO run are provided in Section 5. Section 6 concludes the paper.

2 MODEL DESCRIPTION

The considered example for a climate model is a one-dimensional marine ecosystem model (Oschlies and Garcon, 1999) driven by pre-computed ocean circulation data. In the following, we briefly describe the high-fidelity model and its low-fidelity counterpart which is a basis to construct a surrogate for further use in the optimization process.

2.1 The High-fidelity Model

Simulating the marine ecosystem has become a key tool for understanding the ocean carbon cycle and its variability. The marine ecosystem contains several biogeochemical quantities (called *tracers*), for example nutrients, phyto- and zooplankton which interact and are moreover transported by the ocean circulation and influenced by temperature and salinity. Thus, ecosystem simulations require modeling and computation of both ocean circulation and biogeochemistry. The underlying continuous models are governed by coupled systems of nonlinear, parabolic PDEs or DAEs, for ocean circulation (ocean models, i.e., Navier-Stokes equations with additional temperature and salinity transport equations) and transport of biogeochemical tracers (marine ecosystem models, i.e., convection- or advection-diffusion-reaction type equations) (Sarmiento and Gruber, 2006).

In ecosystem models, the parameters to be optimized – in the following summarized in the vector **u** – are, for example, growth and dying rates of the tracers and thus appear in the usually nonlinear coupling or interaction terms in the model.
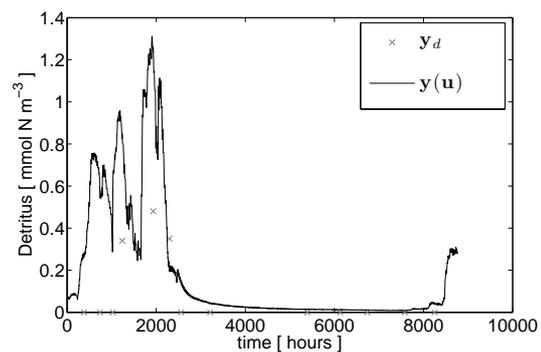

Figure 1: Model response $\mathbf{y}^{(D)}$ (detritus) and observation data $\mathbf{y}_d^{(D)}$ for one year at depth $z \simeq -25\,\mathrm{m}$.

Our example ecosystem model was developed by Oschlies and Garcon (1999) and simulates the interaction of dissolved inorganic nitrogen, phytoplankton, zooplankton and detritus (dead material) – thus also

called *NPZD* model. One aim was to reproduce observations $\mathbf{y}_d$ at different North Atlantic locations by the optimization of model parameters within credible limits. Figure 1 shows the model response and target data, respectively, as illustration for the tracer detritus for a certain depth and a part of the time interval.

The model uses pre-computed ocean circulation and temperature data from an ocean model (in a sometimes called *off-line modus*), i.e., no feedback by the biogeochemistry on the circulation and temperature is modeled (Oschlies and Garcon, 1999).

Since biogeochemistry happens locally and sinking processes only in the vertical water column, we use here a one-dimensional version of the model at a given horizontal position. This is additionally motivated by the fact that there have been special time series studies at fixed locations. Clearly, the computational effort of a one-dimensional simulation is significantly smaller than for the three-dimensional case. Thus, since the one-dimensional case includes all significant features of ecosystem models, it can serve as a good verification example for testing the applicability of surrogate-based approaches that can be later exploited for optimizing the 3D model.

In the *NPZD* model, the concentrations (in mmol N m^{-3}) of dissolved inorganic nitrogen N, phytoplankton P, zooplankton Z, and detritus D are summarized in the vector $y = (y^{(l)})_{l=N,P,Z,D}$ and described by the following coupled PDE system

$$
\left.
\begin{aligned}
\frac{\partial y^{(l)}}{\partial t} &= \frac{\partial}{\partial z}\left(\kappa \frac{\partial y^{(l)}}{\partial z}\right) + \\
&\quad Q^{(l)}(y, u_2, \ldots, u_n), \quad l = N, P, Z \\
\frac{\partial y^{(D)}}{\partial t} &= \frac{\partial}{\partial z}\left(\kappa \frac{\partial y^{(D)}}{\partial z}\right) + \\
&\quad Q^{(D)}(y, u_2, \ldots, u_n) - \frac{\partial y^{(D)}}{\partial z} u_1, \quad l = D
\end{aligned}
\right\} \quad (1)
$$

in $(-H, 0) \times (0, T)$ with additional appropriate initial values. Here, z denotes the only remaining, vertical spatial coordinate, and H the depth of the water column. The terms $Q^{(l)}$ are the biogeochemical coupling (or *source-minus-sink*) terms for the four tracers and $\mathbf{u} = (u_1, \ldots, u_n)$ is the vector of unknown physical and biological parameters. The sinking term is only apparent in the equation for detritus. In the one-dimensional model no advection term is used, since a reduction to vertical advection would make no sense. Thus, the circulation data (taken from an ocean model) are the turbulent mixing coefficient $\kappa = \kappa(z,t)$ and the temperature $\Theta = \Theta(z,t)$, which goes into the nonlinear coupling terms $Q^{(l)}$ but is omitted in the notation.

The continuous model (1) is discretized and solved using an operator splitting method (Marchuk, 1982), an explicit euler timestepping scheme for the nonlinear coupling term Q and the sinking term while using an implicit euler timestepping scheme for the diffusion term. For further details we refer the reader to (Prieß et al., 2011).

In the original model, the time step denoted by τ, is chosen as one hour. The model with this particular time step will be referred to as the high-fidelity or fine one.

In the following, we will denote by $\mathbf{y}_j \approx y(\cdot, t_j)$ the discrete fine model solution of the continous model (1) in time step j (containing all tracers N, P, Z, D) given as

$$\mathbf{y}_j = (y_{ji})_{i=1,\ldots,I}, \quad j = 1, \ldots, M, \quad \mathbf{y} \in \mathbb{R}^{MI} \quad (2)$$

where $I = 66 \times 4$ denotes the number of spatial discrete points for all tracers given by 66, the number of spatial discrete points per tracer, times 4, the number of tracers (cf. (1)) and where $M = 8760$ time steps/year $\times$ 5 years denotes the number of discrete time steps for each tracer.

2.2 Low-fidelity Model

The low-fidelity (or coarse) model, which is a less accurate but computationally cheap representation of $\mathbf{y}$ is obtained by using a coarser time discretization $\hat{\tau}$ given as

$$\hat{\tau} = \beta \tau \quad (3)$$

with a *coarsening factor* $\beta \in \mathbb{N} \setminus \{0, 1\}$, while keeping the spatial discretization fixed. The state variable for this coarser discretized model will be denoted by $\hat{\mathbf{y}}$, the corresponding number of discrete time steps by $\hat{M} = M/\beta$, i.e., we have

$$\hat{\mathbf{y}}_j = (\hat{y}_{ji})_{i=1,\ldots,I}, \quad j = 1, \ldots, \hat{M}, \quad \hat{\mathbf{y}} \in \mathbb{R}^{\hat{M}I}. \quad (4)$$

Note that the parameters $\mathbf{u}$ for this coarse model are the same as for the fine model.

The low-fidelity model is used to create the surrogate of the high-fidelity model, subsequently exploited to optimize the latter at a low computational cost (cf. Section 4).

3 OPTIMIZATION PROBLEM

The key task in parameter optimization is to minimize a least-squares type cost function measuring the misfit between the discrete model output $\mathbf{y} = \mathbf{y}(\mathbf{u})$ and given observational data $\mathbf{y}_d$ (Banks and Kunisch, 1989; Tarantola, 2005). In most cases, the problem is

constrained by parameter bounds. Thus the parameter optimization problem can be written as

$$\min_{\mathbf{u} \in U_{ad}} J(\mathbf{y}(\mathbf{u})) \qquad (5)$$

where

$$J(\mathbf{y}) := \frac{1}{2} \| \mathbf{y} - \mathbf{y}_d \|^2,$$

$$U_{ad} := \{ \mathbf{u} \in \mathbb{R}^n : \mathbf{b}_l \leq \mathbf{u} \leq \mathbf{b}_u \},$$

$$\mathbf{b}_l, \mathbf{b}_u \in \mathbb{R}^n, \quad \mathbf{b}_l < \mathbf{b}_u.$$

The inequalities in the definition of the set U_{ad} of admissible parameters are meant component-wise. The functional J may additionally include a regularization term for the parameters, which was not necessary in our case.

Additional constraints on the state variable $\mathbf{y}$ might be necessary, e.g., to ensure non-negativity of the temperature or of the concentrations of biogeochemical quantities. In our example model however, by using appropriate parameter bounds $\mathbf{b}_l$ and $\mathbf{b}_u$, non-negativity of the state variables can be ensured. This was already observed and used in (Rückelt et al., 2010).

4 SURROGATE-BASED OPTIMIZATION

For many nonlinear optimization problems, a high computational cost of evaluating the objective function and its sensitivity, and, in some cases, the lack of sensitivity information, is a major bottleneck. The need for decreasing the computational cost of the optimization process is especially important while handling complex three-dimensional models.

Surrogate-based optimization (Bandler et al., 2004; Forrester and Keane, 2009; Leifsson and Koziel, 2010; Queipo et al., 2005) is a methodology that addresses these issues by replacing the original high-fidelity model $\mathbf{y}$ by a surrogate, in the following denoted by $\mathbf{s}$, a computationally cheap and yet reasonably accurate representation of $\mathbf{y}$.

Surrogates can be created by approximating sampled high-fidelity model data (*functional* surrogates). Popular techniques include polynomial regression, kriging, artificial neural networks and support vector regression (Queipo et al., 2005; Smola and Schölkopf, 2004; Simpson et al., 2001). Another possibility, exploited in this work, is to construct the surrogate model through appropriate correction/alignment of a low-fidelity or coarse model (*physically-based* surrogates) (Søndergaard, 2003). The advantage of

physically-based surrogates is that a reasonable accuracy can be obtained using a limited number of high-fidelity model data. Also, generalization capability of the physically-based models is typically much better than for functional ones. The specific correction technique exploited in this work is described below.

The surrogate model is updated at each iteration k of the optimization algorithm, typically using available high-fidelity model data. The next iterate, $\mathbf{u}_{k+1}$, is obtained by optimizing the surrogate $\mathbf{s}_k$, i.e.,

$$\mathbf{u}_{k+1} = \arg\min_{\mathbf{u} \in U_{ad}} J(\mathbf{s}_k(\mathbf{u})). \qquad (6)$$

Then, the updated surrogate $\mathbf{s}_{k+1}$ is determined by re-aligning the low-fidelity model at $\mathbf{u}_{k+1}$ and optimized again as in (6). The process of aligning the coarse model to obtain the surrogate and subsequent optimization of this surrogate is repeated until a user-defined termination condition is satisfied.

If the surrogate $\mathbf{s}_k$ satisfies so-called zero-order and first-order consistency conditions (Conn et al., 2000; Koziel et al., 2010) with the high-fidelity model at $\mathbf{u}_k$, i.e., $\mathbf{s}_k(\mathbf{u}_k) = \mathbf{y}(\mathbf{u}_k)$, $\mathbf{s}_k'(\mathbf{u}_k) = \mathbf{y}'(\mathbf{u}_k)$ the surrogate-based scheme (6) is provably convergent to at least a local optimum of (5), provided that both the low- and high-fidelity models are sufficiently smooth, and the surrogate optimization step is enhanced by the the trust-region (TR) safeguard (Conn et al., 2000; Koziel et al., 2010). The surrogate model utilized in this work only satisfies the zero-order consistency with the high-fidelity model. Still, as demonstrated in Section 5, the performance of our surrogate-based optimization process is satisfactory even without using the trust-region convergence safeguards.

4.1 Surrogate Model using Basic Multiplicative Response Correction

The multiplicative response correction is one reasonable way to construct a physically-based surrogate for the marine ecosystem model given in Section 2.1. This approach was successfully exploited in (Prieß et al., 2011), and it is briefly recalled below.

The surrogate response $\mathbf{s}_k(\mathbf{u})$, at iteration k of the optimization process, is generated by multiplicative correction of the *smoothed* low-fidelity model response (cf. Subsection 2.2), denoted by $\tilde{\mathbf{y}}$, yielding

$$s_{kji}(\mathbf{u}) := A_{kji} \, \tilde{\tilde{y}}_{ji}(\mathbf{u}), \qquad \left. \begin{array}{l} k = 1, 2, \ldots \\ j = 1, \ldots, \hat{M} \\ i = 1, \ldots, I \\ \beta = M/\hat{M} \end{array} \right\} \qquad (7)$$

$$A_{kji} := \frac{\tilde{y}_{ji}^{\beta}(\mathbf{u}_k)}{\tilde{\tilde{y}}_{ji}(\mathbf{u}_k)}$$

where A_{kji} denotes the *correction factor* given as the point wise division of the smoothed and *down-sampled* fine model response, denoted by $\tilde{\mathbf{y}}^{\beta}$, by the
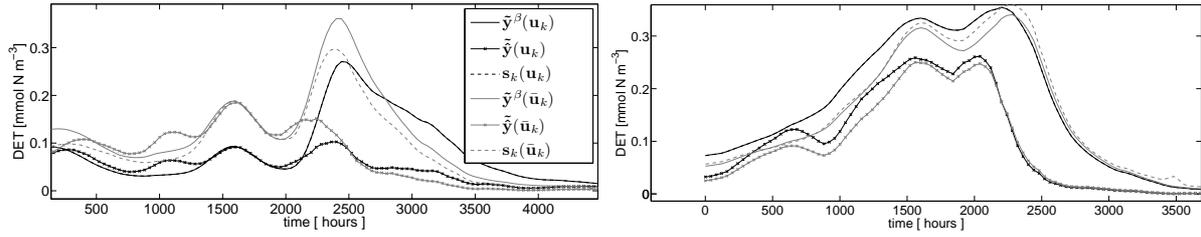
Figure 2: Surrogate's, fine (down-sampled, smoothed) and coarse (smoothed) model responses $\mathbf{s}_k, \tilde{\mathbf{y}}^\beta$ and $\tilde{\mathbf{y}}$ for the tracer detritus (at depth $z \approx -2.68\,\mathrm{m}$) at two points $\mathbf{u}_k$ and corresponding perturbations $\bar{\mathbf{u}}_k$ (see the text for details). The surrogate, established at $\mathbf{u}_k$, is perfectly aligned with the fine model at $\mathbf{u}_k$ and provides a reasonable approximation of the fine model response at $\bar{\mathbf{u}}_k$. For illustration, only the model responses for one representative tracers, depth layer, and a part of the whole time interval is shown.

smoothed coarse model response at the point $\mathbf{u}_k$. This simple correction scheme is justified by the fact that the overall "shape" of the low-fidelity model response resembles that of the high-fidelity one.

It was observed that smoothing allows us to remove the numerical noise from the coarse model response and identify the main characteristics of the traces of interest. Consequently, also the (down-sampled) fine model response is smoothed in (7), yielding $\tilde{\mathbf{y}}^\beta$, before calculating the multiplicative correction factor. Sampling of the fine model response was necessary to make it commensurable with the corresponding coarse model response. The sampled fine model response $\mathbf{y}^\beta$ is given as

$$y_{ji}^\beta := y_{\beta j, i}, \quad j = 1, \ldots, \hat{M}, \quad i = 1, \ldots, I,$$

$$\mathbf{y}^\beta \in \mathbb{R}^{\hat{M}I}. \tag{8}$$

The correction step in iteration k on the whole discrete state vector is given as

$$\mathbf{s}_k(\mathbf{u}) := A_k \circ \tilde{\mathbf{y}}(\mathbf{u}), \quad \mathbf{s}_k \in \mathbb{R}^{\hat{M}I},$$

$$A_k := \left(A_{kji}\right)_{j,i} \in \mathbb{R}^{\hat{M} \times I} \tag{9}$$

where A_k, the *correction matrix* in step k, and the operation "$\circ$" are defined by (7).

By definition the surrogate model is zero-order consistent with the (down-sampled and smoothed) fine model in the point $\mathbf{u}_k$ (i.e. $\mathbf{s}_k(\mathbf{u}_k) \approx \tilde{\mathbf{y}}^\beta(\mathbf{u}_k)$). As we do not use sensitivity information, the first-order consistency condition cannot be satisfied exactly. Nevertheless, as was shown in (Prieß et al., 2011), this surrogate model exhibits quite good generalization capability, which means that the surrogate provides a reasonable approximation of the high-fidelity one in the neighborhood of $\mathbf{u}_k$.

Figure 2 shows the surrogate's, fine (down-sampled) and coarse model responses $\tilde{\mathbf{y}}^\beta, \tilde{\mathbf{y}}, \mathbf{s}_k$ at two different points, $\mathbf{u}_k$ and $\bar{\mathbf{u}}_k$. The surrogate model is

established at $\mathbf{u}_k$ and, therefore, its output is perfectly aligned with the fine model output at $\mathbf{u}_k$. The surrogate model prediction is still good at $\bar{\mathbf{u}}_k$. Since the distance between subsequent iterations points normally decrease upon convergence of the optimization algorithm, the prediction of the surrogate model is becoming more and more accurate towards the end of the optimization run.

4.2 Difficulties of Basic Surrogate Formulation

Occasionally, when using the surrogate given in (7), there might occur a situation where the coarse model response is close to zero (and maybe even negative due to approximation errors) and a few magnitudes smaller than the fine one, which leads to large (possibly negative) entries in the corresponding correction tensor A_k. While such a correction tensor ensures zero-order consistency at the point where it was established (i.e., $\mathbf{u}_k$), it may lead to (locally) poor approximation in the vicinity of $\mathbf{u}_k$.

Figure 3 (left) illustrates these issues by showing the smoothed surrogate's, fine (down-sampled) and coarse model responses $\tilde{\mathbf{y}}^\beta, \tilde{\mathbf{y}}, \mathbf{s}_k$ for the state detritus at one illustrative time interval and depth layer. Shown are the model responses at the same iterations $\mathbf{u}_k$ and its neighborhood $\bar{\mathbf{u}}_k \in B_\delta(\mathbf{u}_k)$ as in Figure 2.

It should be pointed out that the overall shape of the surrogate's response provides a reasonable approximation of the fine model response (and more accurate than the corresponding coarse model response) despite of the distortion illustrated in Figure 3. This is supported by the fact that even without addressing these issues, the surrogate-based scheme (6) was able to yield satisfactory results, not only with respect to the quality of the final solution, but, most importantly, in terms of the low computational cost of the optimization process. This was demonstrated in (Prieß et al., 2011).
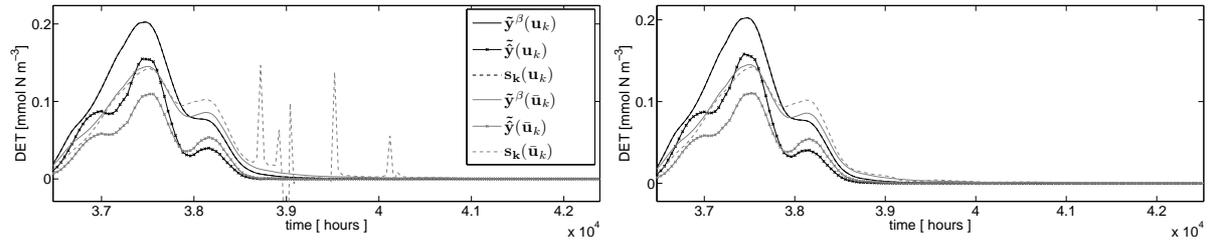
Figure 3: Surrogate's, fine (down-sampled, smoothed) and coarse (smoothed) model responses $\mathbf{s}_k, \tilde{\mathbf{y}}^\beta$ and $\tilde{\tilde{\mathbf{y}}}$ for the same representative tracer, depth layer and parameter vectors $\mathbf{u}_k$ and $\bar{\mathbf{u}}_k$ as in Figure 2 while showing a different time interval. Using the basic surrogate formulation (9), possible large positive and negative entries in the corresponding correction tensor A_k may lead to (locally) poor approximation of the resulting surrogate in the vicinity of $\mathbf{u}_k$ (left). However, the overall shape of the surrogate still provides a reasonable approximation of the fine one (and more accurate than the corresponding coarse model response). Employing the improvements in (10) the large positive and negative peaks are removed (right). See the text for details.

4.3 Improved Response Correction Scheme

The response distortion described in the previous section is problematic towards the end of the surrogate-based optimization run when the small changes of the model parameters and the corresponding responses are considered. The "'spikes'" appearing in the response due to large values of the correction term can be viewed, in a way, as a numerical noise that slows down the algorithm convergence and makes the optimum more difficult to locate.

A few simple means described below can address these issues and further improve the accuracy of the surrogate's response as well as the performance of the optimization algorithm.

We introduce non-negative bounds for the coarse model response (the negative response is non-physical and is a result of numerical errors due to using large time steps in the coarse model), upper bounds for the correction factor as well as restrict the correction factor to one in case the fine and coarse model responses are below a certain threshold ε. Here, we use $\varepsilon = 10^{-10}$. More specifically, the following modifications of the model outputs and the scaling factors are performed for each iteration k, discrete time step j and depth layer i:

$$(i) \ \hat{y}_{ji}(\mathbf{u}_k) = \max\{\, \hat{y}_{ji}(\mathbf{u}_k), 1e - 8 \,\}$$

$$(ii) \ A_{kji} = \min\{\, A_{kji}, 10 \,\} \qquad (10)$$

$$(iii) \ A_{kji} = 1 \text{ if } \left(\tilde{y}_{ji}^\beta(\mathbf{u}_k) \le \varepsilon \text{ and } \tilde{\tilde{y}}_{ji}(\mathbf{u}_k) \le \varepsilon \right)$$

where (i) is employed before smoothing the coarse model response.

Figure 3 (right) shows the surrogate's, fine (down-sampled) and coarse model response for the same illustrative tracer, time interval and depth layer as Fig-

ure 3 (left), however, while employing the improvements given in (10). It can be observed that the large positive and negative peaks present in the surrogate responses of Figure 3 (left) are removed after applying (10).

The numerical results presented in Section 5 demonstrate that this improved response correction scheme allows us to further improve the computational efficiency of the surrogate-based scheme (6).

5 NUMERICAL RESULTS

The optimization setup used in this work is the following. For all optimization runs we use the MATLAB[1] function fmincon, exploiting the active-set algorithm. The following cost functions

$$J(\mathbf{z}) := ||\mathbf{z} - \mathbf{y}_d||^2 = \sum_{i=1}^{I} \sum_{j=1}^{\hat{M}} (z_{ji} - (y_d)_{ji})^2, \quad (11)$$

$$\tilde{J}(\mathbf{z}) := ||\mathbf{z} - \tilde{\mathbf{y}}_d||^2 = \sum_{i=1}^{I} \sum_{j=1}^{\hat{M}} (z_{ji} - (\tilde{y}_d)_{ji})^2, \quad (12)$$

$$(y_d)_{ji} := y_{ji}^\beta(\mathbf{u}_d), \quad \mathbf{z} \in \mathbb{R}^{\hat{M}I}$$

were used for the fine model optimization ((11) with $\mathbf{z} = \mathbf{y}^\beta$), for the coarse model ((12) with $\mathbf{z} = \tilde{\mathbf{y}}$) and surrogate optimization ((12) with $\mathbf{z} = \mathbf{s}_k$), whereas (11) was used in the termination condition and to compare the results. The down-sampled fine model output is given by (8) and the target data $\mathbf{y}_d$ – as a first illustration – was synthetically created by the (down-sampled) fine model output at parameter vector $\mathbf{u}_d$. Sampling was necessary to yield a comparable fine

---

[1]MATLAB is a registered trademark of The MathWorks, Inc., http://www.mathworks.com
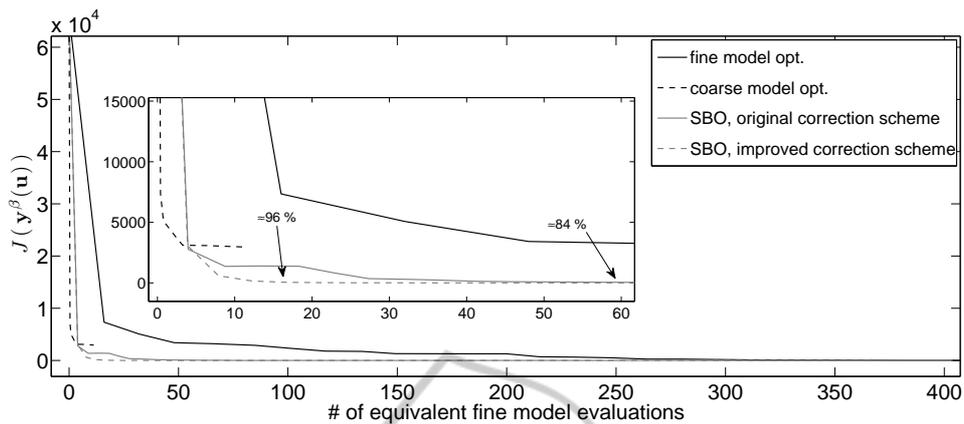
Figure 4: Values of the cost function J (cf. (11)) versus the equivalent number of fine model evaluations for a SBO run using the surrogate model exploiting the original (cf. (7)) and the improved correction scheme (cf. (10)), as well as for a fine and coarse model optimization run. The figure also indicates those points in the SBO runs that correspond to a termination condition of $J(\mathbf{y}^\beta(\mathbf{u}_k)) \leq 50$, ensuring good visual agreement between the fine model output and the target. After employing the improvements suggested in (10), the number of equivalent fine model evaluations required to satisfy this termination condition was reduced from 60 down to only 17, resulting in an increase of the corresponding time savings, from 84% to about 96%, when compared to the direct fine model optimization.

model optimization run while in (12) smoothing of the target data is performed since smoothing of the coarse model and surrogate's response was employed in the corresponding optimization runs.

For the sake of comparison, we run the direct fine and coarse model optimizations as well as the surrogate-based algorithm (cf. (6)) exploiting the original and improved response correction scheme (7) and (10).

Results are presented in Figure 4 showing the value of the cost function J (cf. (11)) versus the equivalent number of fine model evaluations for the SBO algorithm using the surrogate model exploiting the original and the improved correction scheme, as well as for the fine and coarse model optimization (Prieß et al., 2011). Equivalent fine model evaluations are determined taking into account the coarsening factor β. More specifically, one evaluation of the coarse model with a coarsening factor β is equivalent to $1/\beta$ evaluations of the fine model. The total optimization cost is calculated as $n_f + n_c/\beta$, where n_f (n_c) denotes the overall number of fine (coarse) model evaluations during the optimization run. Recall that SBO scheme 6 requires one fine model evaluation per algorithm iteration.

Figure 4 indicates the points in the SBO run that correspond to a termination condition of $J(\mathbf{y}^\beta(\mathbf{u}_k)) \leq 50$. This particular value was selected as it ensures good visual agreement between the fine model output and the target.

Figure 5 shows the down-sampled fine model response for the optimal parameter values obtained us-

ing the SBO algorithm with the original and improved response correction scheme (denoted by $\mathbf{u}_{s,1}^*, \mathbf{u}_{s,2}^*$). Only two tracers at a certain depth level and time interval are included for illustration. For the sake of completeness the responses obtained through the direct fine and coarse model optimization, denoted by $\mathbf{u}^*, \hat{\mathbf{u}}^*$, are also included.

It should be noted that the model parameters obtained by directly optimizing the coarse model result in a cost function value of $J(\mathbf{y}^\beta(\hat{\mathbf{u}}^*)) \approx 2960$ (optimization cost: 11 equivalent fine model evaluations) (cf. Figure 4). This solution is far away from that obtained by the direct fine model optimization (cf. Figure 5), which indicates that the coarse model is not a reliable prediction tool.

Direct fine model optimization yields a very low cost function of $J(\mathbf{y}^\beta(\hat{\mathbf{u}}^*)) \approx 1.267 \cdot 10^{-2}$, corresponding to a solution close to the target data (cf. Figure 5). However, the optimization cost is substantially higher: 983 fine model evaluations. Note that for better readability, Figure 4 only shows the range 0-400 function evaluations.

In (Prieß et al., 2011), we demonstrated that in the SBO run based on the original response correction scheme (7), the chosen termination condition $J(\mathbf{y}^\beta(\mathbf{u}_k)) \leq 50$ could be reached after approximately 60 equivalent fine model evaluations. This resulted in a reduction of the total optimization cost of about 84% when compared to the fine model optimization (the direct fine model optimization required 375 evaluations to reach this cost function value, cf. Figure 4).
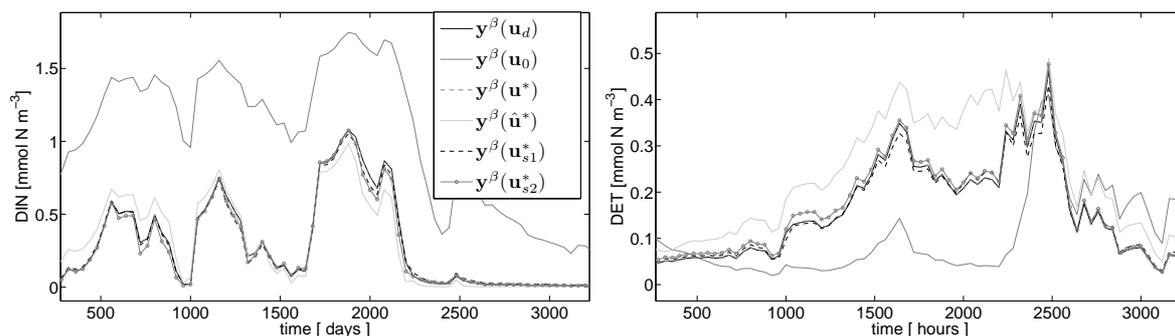
After employing the improvements suggested in

455

Figure 5: Fine model output $\mathbf{y}^{\beta}$ (down-sampled) for state dissolved inorganic nitrogen (left) and the state detritus (right) at depth $z \approx -2.68\,\mathrm{m}$. Shown are, in the legend from top to bottom: (i) Target $\mathbf{y}_d$, (ii) fine model output at the initial value $\mathbf{u}_0$, (iii) at the result of the direct fine model optimization yielding $\mathbf{u}^*$, (iv) at the coarse model optimum $\hat{\mathbf{u}}^*$ and (iv), (v) at the optima $\mathbf{u}_{s1}^*, \mathbf{u}_{s2}^*$ obtained by the surrogate-based algorithm (6) exploiting the original (cf. (7)) and the improved (cf. (10)) response correction scheme. Solutions (iv) and (v) are both very close to (iii) but the solution (v) was obtained at the computational cost three times lower than (iv).

(10), only 17 equivalent fine model evaluations were required to satisfy the same termination condition, which is over three times less than for the original response correction scheme. The corresponding reduction of the total optimization cost, compared to the direct fine model optimization, is about 96% (cf. Figure 4). The corresponding solution is close to that obtained by direct fine model optimization as shown in Figure 5.

6 CONCLUSIONS

Parameter optimization in climate models can be very expensive in terms of the cost function and gradient evaluations, especially for three-dimensional cases. Therefore, methods that aim at reducing the optimization cost of such high-fidelity (fine) models, such as surrogate-based optimization (SBO) techniques, are highly desirable. Here, the idea is to replace the fine model in the optimization run by a surrogate, a computationally cheap and yet reasonably accurate representation.

As a case study, we are interested in a parameter optimization of a one-dimensional representative of a class of marine ecosystem models. It follows that a simple multiplicative response correction applied to a temporarily coarser discretized physics-based low-fidelity (coarse) model of the system of interest is sufficient to create a reliable surrogate of the original, high-fidelity ecosystem model. This approach allowed us to yield remarkably good results, both in terms of the quality of the final solution and, most importantly, in terms of the relative reduction in the total optimization cost, about 84% when compared to the direct fine model optimization.

In this paper, we demonstrated that the correction scheme can be enhanced to alleviate the difficulties of its original version, which results in further improvement of the surrogate model accuracy and overall performance of the optimization algorithm utilizing this surrogate. The optimization cost was reduced by a factor of three (from 16% to 5% of the direct high-fidelity model optimization optimization cost), which corresponds to the cost savings of 95%.

ACKNOWLEDGEMENTS

REFERENCES

Bandler, J. W., Cheng, Q. S., Dakroury, S. A., Mohamed, A. S., Bakr, M. H., Madsen, K., and Søndergaard, J. (2004). Space mapping: The state of the art. *IEEE T. Microw. Theory.*, 52(1).

Banks, H. T. and Kunisch, K. (1989). *Estimation Techniques for Distributed Parameter Systems*. Birkhäuser.

Conn, A. R., Gould, N. I. M., and Toint, P. L. (2000). *Trust-region methods*. Society for Industrial and Applied Mathematics, Philadelphia, PA.

Fennel, W. and Neumann, T. (2004). *Introduction to the Modelling of Marine Ecosystems*. Elsevier.

Forrester, A. I. and Keane, A. J. (2009). Recent advances in surrogate-based optimization. *Prog. Aerosp. Sci.*, 45(1-3):50–79.

Gill, A. E. (1982). *Atmosphere - Ocean Dynamics*, volume 30 of *International Geophysics Series*. Academic Press.

Koziel, S., Bandler, J. W., and Cheng, Q. S. (2010). Robust trust-region space-mapping algorithms for microwave design optimization. *IEEE T. Microw. Theory.*, 58(8):2166–2174.

Leifsson, L. and Koziel, S. (2010). Multi-fidelity design optimization of transonic airfoils using physics-based surrogate modeling and shape-preserving response prediction. *Journal of Computational Science*, 1(2):98–106.

Majda, A. (2003). *Introduction to PDE's and Waves for the Atmosphere and Ocean*. AMS.

Marchuk, G. I. (1982). *Methods of Numerical Mathematics*. Springer, 2nd edition.

McGuffie, K. and Henderson-Sellers, A. (2005). *A Climate Modelling Primer*. Wiley, 3nd edition.

Oschlies, A. and Garcon, V. (1999). An eddy-permitting coupled physical-biological model of the north atlantic. 1. sensitivity to advection numerics and mixed layer physics. *Global Biogeochem. Cy.*, 13:135–160.

Prieß, M., Koziel, S., and Slawig, T. (2011). Surrogate-based optimization of climate model parameters using response correction. Preprint 1104, Christian-Albrechts-Universität zu Kiel, Institute for Computer Science.

Queipo, N. V., Haftka, R. T., Shyy, W., Goel, T., Vaidyanathan, R., and Tucker, P. K. (2005). Surrogate-based analysis and optimization. *Prog. Aerosp. Sci.*, 41(1):1–28.

Rückelt, J., Sauerland, V., Slawig, T., Srivastav, A., Ward, B., and Patvardhan, C. (2010). Parameter optimization and uncertainty analysis in a model of oceanic co2-uptake using a hybrid algorithm and algorithmic differentiation. *Nonlinear Analysis: Real World Applications*, online.

Sarmiento, J. and Gruber, N. (2006). *Ocean Biogeochemical Dynamics*. Princeton University Press.

Simpson, T., Poplinski, J., Koch, P. N., and Allen, J. (2001). Metamodels for computer-based engineering design: Survey and recommendations. *Eng. Comput.*, 17:129–150. 10.1007/PL00007198.

Smola, A. J. and Schölkopf, B. (2004). A tutorial on support vector regression. *Stat. Comput.*, 14:199–222. 10.1023/B:STCO.0000035301.49549.88.

Søndergaard, J. (2003). *Optimization using surrogate models - by the space mapping technique*. PhD thesis, Informatics and Mathematical Modelling, Technical University of Denmark, DTU, Richard Petersens Plads, Building 321, DK-2800 Kgs. Lyngby. Supervisor: Kaj Madsen.

Tarantola, A. (2005). *Inverse Problem Theory and Methods for Model Parameter Estimation*. SIAM.